

TPR – 01 – 04
hep-ph/0103275

QCD factorization for the pion diffractive dissociation to two jets

V.M. BRAUN¹, D.YU. IVANOV^{1,2} A. SCHÄFER¹ and L. SZYMANOWSKI^{1,3}

¹*Institut für Theoretische Physik, Universität Regensburg,
D-93040 Regensburg, Germany*

²*Institute of Mathematics, 630090 Novosibirsk, Russia*

³*Soltan Institute for Nuclear Studies, Hoza 69,
00-681 Warsaw, Poland*

Abstract:

We calculate the cross section of a pion diffraction dissociation in two jets with large transverse momenta originating from a hard gluon exchange between the pion constituents. To the leading logarithmic accuracy (in energy), the contribution coming from small transverse separations between the quark and the antiquark in the pion acquires the expected factorized form, the longitudinal momentum distribution of the jets being proportional to the pion distribution amplitude. The hard gluon exchange can in this case be considered as a part of the unintegrated gluon distribution. Beyond the leading logarithms (in energy) this proportionality does not hold. Moreover, the collinear factorization appears to be broken by the end-point singularities. Remarkably enough, the longitudinal momentum distribution of the jets for the non-factorizable contribution is calculable, and turns out to be the same as for the factorizable contribution with the asymptotic pion distribution amplitude.

1. It has been conjectured a long time ago [1] that pion diffraction dissociation on a heavy nucleus $\pi A \rightarrow X A$ is sensitive to small transverse size configurations of pion constituents. It was later argued [2, 3] that selecting a specific hadronic final state that consists of a pair of (quark) jets with large transverse momentum $q_{1\perp} \simeq -q_{2\perp}$ one can obtain important insight into the pion structure as it turns out that the longitudinal momentum fraction distribution of the jets follows that of the pion valence parton constituents. A measurement of hard dijet coherent production on nuclei presents, therefore, the exciting possibility of a direct measurement of the pion distribution amplitude and provides striking evidence [4] that this distribution is close to its asymptotic form.

From the theoretical point of view, the principal question is whether the relevant transverse size of the pion r_\perp (alias the scale of the pion distribution amplitude $\mu = 1/r_\perp$) is determined by the color transparency condition $\mu \sim A^{1/3} \Lambda_{\text{QCD}}$ or whether it is of the order of the transverse momenta of the jets $\mu \sim q_\perp$. In the latter case one could envisage a factorization formula for the amplitude of hard dijet coherent production of the type (cf. Fig. 1)

$$\mathcal{M}_{\pi \rightarrow 2 \text{ jets}} = \int_0^1 dz' \int_0^1 dx_1 \phi_\pi(z', \mu_F^2) T_H(z', x_1, \mu_F^2) F_\zeta^g(x_1, \mu_F^2). \quad (1)$$

Here $\phi_\pi(z', \mu_F^2)$ is the pion distribution amplitude, and $F_\zeta^g(x_1, \mu_F^2)$ is the non-forward (skewed) gluon distribution [5, 6] in the target nucleon or nucleus; x_1 and $x_2 = x_1 - \zeta$ are the momentum fractions of the emitted and the absorbed gluons, respectively. (The asymmetry parameter ζ is fixed by the process kinematics, see below.) $T_H(z', x_1, \mu_F^2)$ is the hard scattering amplitude and μ_F is the (collinear) factorization scale.

To the best of our knowledge, this question has never been studied. As a first step in this direction, in this letter we present an explicit calculation of the leading-order contribution to the imaginary part of $T_H(z', x_1, \mu_F^2)$ corresponding to a single hard gluon exchange. Since we are not interested in the color transparency phenomena, we restrict ourselves to scattering from a single nucleon. We will find that the structure of the hard gluon exchange is such that it generates an enhancement by a logarithm of the energy in the region $z' \simeq z$ where z is the energy fraction carried by the (quark) jet. If only this logarithmic contribution is retained, the longitudinal momentum distribution of the jets indeed follows the shape of the pion distribution amplitude [2, 3]. The hard gluon exchange can in this case be considered as a part of the unintegrated gluon distribution, as advocated in [3]. Beyond the leading logarithms (in energy) this proportionality does no longer hold. Moreover, the collinear factorization (1) appears to be broken by the end-point singularities. Remarkably enough, the longitudinal momentum distribution of the jets for the non-factorizable contribution is calculable, and turns out to be the same as for the factorizable contribution with the asymptotic pion distribution amplitude.

2. The kinematics of the process is shown in Fig. 1. For definiteness, we consider pion scattering from a nucleon target. The momenta of the incoming pion, incoming nucleon and the outgoing nucleon are p_1, p_2 and p'_2 , respectively. The pion and the nucleon masses are both neglected, $p_1^2 = 0, p_2^2 = (p'_2)^2 = 0$. We denote the momenta of

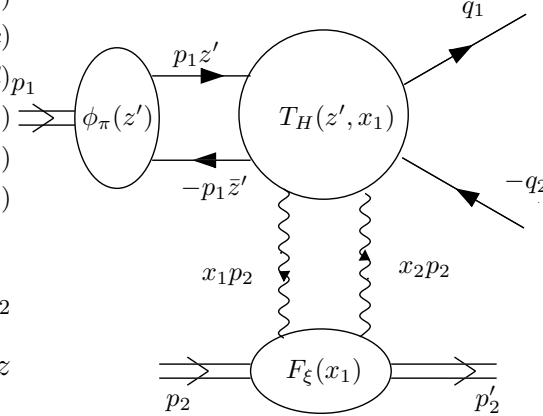


Figure 1: Kinematics of the coherent hard dijet production $\pi \rightarrow 2$ jets. The hard scattering amplitude T_H contains at least one hard gluon exchange.

the outgoing quark and antiquark (jets) as q_1 and q_2 , respectively. They are on the mass shell, $q_1^2 = q_2^2 = 0$. We will use the Sudakov decomposition of 4-vectors with respect to the momenta of the incoming particles p_1 and p_2 . For instance, the jet momenta are decomposed according to

$$q_1 = zp_1 + \frac{q_{1\perp}^2}{zs}p_2 + q_{1\perp}, q_2 = \bar{z}p_1 + \frac{q_{2\perp}^2}{\bar{z}s}p_2 + q_{2\perp} \quad (2)$$

such that z is the longitudinal momentum fraction of the quark jet in the lab frame. We will often use the shorthand notation: $\bar{u} \equiv (1 - u)$ for any longitudinal momentum fraction u . The Dirac spinors for the quark and the antiquark are denoted by $u(q_1)$ and $v(q_2)$.

We are interested in the forward limit, when the transferred momentum $t = (p_2 - p_2')^2$ is equal to zero*, and the transverse momenta of jets compensate each other $q_{1\perp} \equiv q_\perp$, $q_{2\perp} \equiv -q_\perp$. In this kinematics the invariant mass of the produced $q\bar{q}$ pair is equal to $M^2 = q_\perp^2/z\bar{z}$. The invariant c.m. energy $s = (p_1 + p_2)^2 = 2p_1p_2$ is taken to be much larger than the transverse jet momentum q_\perp . In what follows we neglect contributions to the amplitude that are suppressed by powers of $1/s$.

The general scheme of the calculation can be explained as follows. Since the hard scattering amplitude $T_H(z', x_1, \mu_F^2)$, by assumption, does not depend on the target, we choose to consider the hard dijet production from a quark, $\pi q \rightarrow (\bar{q}q)q$. We replace the pion by a collinear $\bar{q}q$ pair with the momenta $z'p_1$ and $\bar{z}'p_1$, respectively. The probability amplitude to find a particular value of the momentum fraction z' is given by the pion distribution amplitude defined as

$$\langle 0 | \bar{d}(y) \gamma_\mu \gamma_5 u(-y) | \pi^+(p) \rangle_{y^2 \rightarrow 0} = i p_\mu f_\pi \int_0^1 dz' e^{i(2z' - 1)(py)} \phi_\pi(z'), \quad (3)$$

*If the target mass m is taken into account, the momentum transfer $t = (p_2 - p_2')^2$ contains a non-vanishing longitudinal contribution and is constrained from below by $|t| \geq t_0$, where $t_0 = (m^2 M^4)/(s - m^2)^2$, M^2 being the invariant mass of the dijet.

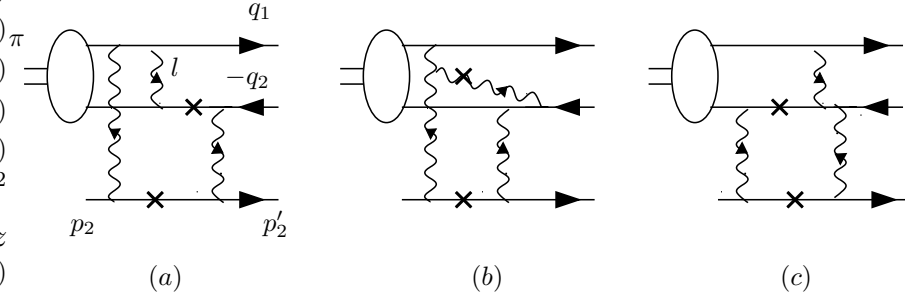


Figure 2: Cut diagrams (examples) for the imaginary part of the amplitude $\pi q \rightarrow (\bar{q}q)q$. The cut quark (gluon) propagators are indicated by crosses.

where $f_\pi \simeq 131$ MeV is the pion decay constant. Light-cone dominance for the t -channel gluon emission is not assumed from the beginning, but has to follow from the calculation in order that the result can be interpreted in the sense of the factorization formula (1). To this end, the gluon transverse momentum k_\perp is kept nonzero and we show that the amplitude in question contains a collinear logarithm $\ln q_\perp^2/\mu_F^2$ coming from the integration region $\mu_F^2 \ll k_\perp^2 \ll q_\perp^2$. This property allows to calculate the upper part of the diagrams represented schematically in Fig. 1 assuming that $k_\perp^2 \ll q_\perp^2$ i.e. in the light-cone limit. In the last step, the collinear logarithm is interpreted as a contribution to the gluon distribution in the target and the (perturbative) non-forward gluon distribution of the quark is substituted by the (nonperturbative) non-forward gluon distribution in the nucleon.

In this letter we calculate the imaginary part of the amplitude. The real part can in principle be restored from the imaginary part using dispersion relations. One rationale for this procedure is that at high energies the scattering amplitudes corresponding to Pomeron exchange are dominated by their imaginary parts. The second rationale is simplicity: the corresponding cut diagrams (see Fig. 2 for examples) are built of tree-level on-shell scattering amplitudes and their form is strongly constrained by gauge invariance, see below.

The existing cut diagrams can be grouped into the four gauge-invariant contributions shown in Fig. 3a–d, which differ by the position of the hard gluon that provides the large

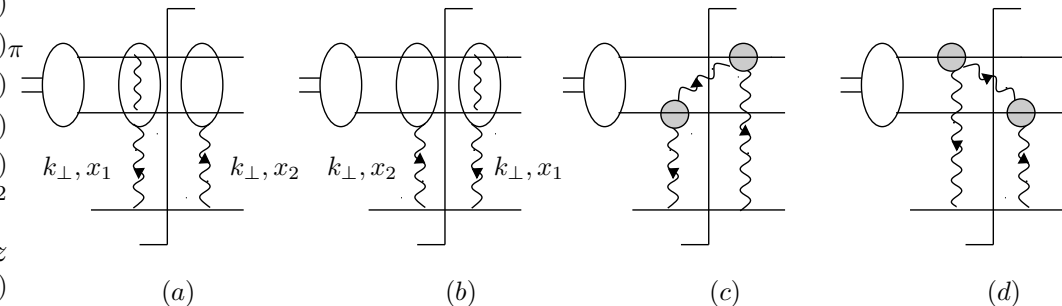


Figure 3: The decomposition of the imaginary part of the amplitude $\pi q \rightarrow (\bar{q}q)q$ into four gauge-invariant contributions.

momentum transfer to the jets. The corresponding contributions to the amplitude will

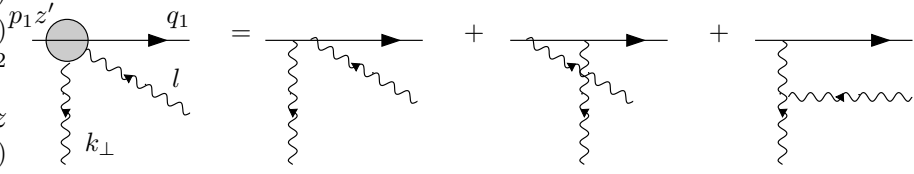


Figure 4: The effective vertex.

be denoted as $\mathcal{M}_{(a)}$, $\mathcal{M}_{(b)}$, $\mathcal{M}_{(c)}$ and $\mathcal{M}_{(d)}$. For example, in Fig. 3a it is assumed that the hard gluon exchange appears to the left of the cut. This contribution is given by the sum of 10 Feynman diagrams one of which is shown in Fig. 2a. Similarly, the contribution in Fig. 3b is given by the sum of 10 diagrams with the hard gluon exchange appearing to the right of the cut; a typical diagram is shown in Fig. 2c. The two remaining contributions in Fig. 3c and Fig. 3d take into account the possibility of real gluon emission in the intermediate state. The filled circles stand for the effective vertices describing the gluon radiation, see Fig. 4. Each of the two contributions in Fig. 3c,d corresponds to a sum of 9 different Feynman diagrams, see Fig. 2b for an example.

We use Feynman gauge and perform the usual substitution

$$g_{\mu\nu} \rightarrow \frac{p_2^\mu p_1^\nu}{(p_1 p_2)} \quad (4)$$

in the propagators of t -channel gluons. This is correct up to terms $\sim 1/s$ which is sufficient for our purposes. The t -channel gluon momenta are expanded according to

$$\begin{aligned} k_1^\mu &= \alpha_1 p_1^\mu + x_1 p_2^\mu + k_\perp^\mu, \\ k_2^\mu &= \alpha_2 p_1^\mu + x_2 p_2^\mu + k_\perp^\mu. \end{aligned} \quad (5)$$

As is easily checked by inspection, in any cut diagram two internal lines are on the mass shell. The corresponding two on-shellness conditions fix α_1 and x_1 and relate the variables z' and x_1 to one other. In addition, α_2 and x_2 are fixed by the energy-momentum conservation. Since $\alpha_{(1,2)}$ and $x_{(1,2)}$ are all of the order of $1/s$, the $1/k_{1,2}^2$ factors in the propagators of the t -channel gluons can be approximated by $k_{(1,2)}^2 = \alpha_{(1,2)} x_{(1,2)} s - k_\perp^2 = -k_\perp^2 + \mathcal{O}(1/s)$. Using the on-shellness conditions for the contributions in Fig. 3a and Fig. 3b one obtains $x_1 = \zeta$, $x_2 = 0$, for any z' . For Fig. 3d one finds $x_1 = \zeta z' \bar{z} / (z' - z)$, $x_2 = \zeta z \bar{z}' / (z' - z)$ and $z' > z$, where the last condition ensures that the energy of the cut gluon is positive. Finally, for the set of cut-diagrams corresponding to Fig. 3c we obtain $x_1 = \zeta z \bar{z}' / (z - z')$, $x_2 = \zeta z' \bar{z} / (z - z')$ and $z > z'$.

After the on-shellness conditions are used, a single integration over the gluons transverse momentum k_\perp remains:

$$\text{Im } \mathcal{M} \sim \int \frac{d^2 k_\perp}{(k_\perp^2)^2} J_{up}(k_\perp, q_\perp) J_{down}(k_\perp, q_\perp), \quad (6)$$

where k_\perp^4 comes from the product of the two gluon propagators. J_{up} and J_{down} are dubbed impact factors and stand for the upper and the lower parts of the diagrams Fig. 2a-d

(connected by the two-gluon exchange). The representation (6) is well known [7, 8] from QED scattering at high energies.

Properties of the impact-factors J_{up} and J_{down} as a functions of k_\perp at $k_\perp \rightarrow 0$ are of crucial importance. Since J_{down} is the impact-factor of a point-like target quark, $J_{down}(k_\perp, q_\perp) \sim const$. On the other hand, $J_{up}(k_\perp, q_\perp)$ stands for the scattering of the colorless $q\bar{q}$ (Fig. 3a–b) or $q\bar{q}G$ (Fig. 3c–d) state having a transverse size $\sim 1/q_\perp$ and has to vanish at small $k_\perp \ll q_\perp$, $J_{up}(k_\perp, q_\perp) \sim k_\perp^2$, as a consequence of the color neutrality of the quark-antiquark pair: A gluon with a large wave length $\sim 1/k_\perp$ cannot resolve a color dipole of the small size $\sim 1/q_\perp$. Since in our case there are two gluons, J_{up} is proportional to the product $k_\perp \cdot k_\perp = k_\perp^2$ [†]. In the opposite limit of large transferred momenta, $k_\perp \gg q_\perp$, the two t –channel gluons are forced to couple to the same parton (quark or gluon) in the upper block in Fig. 3a–d. It follows that at large k_\perp $J_{up}(k_\perp, q_\perp) \sim const$.

Taking into account the above properties of the impact-factors we conclude that the transverse momentum integration in (6) diverges logarithmically at small k_\perp and the integral can be estimated as $\mathcal{M} \sim \int^{q_\perp^2} dk_\perp^2/k_\perp^2 \sim \ln q_\perp^2$, as expected. The region of $k_\perp^2 > q_\perp^2$ does not produce the large logarithm and can be neglected. Note that the correct small k_\perp behavior of the impact factors is only recovered in the sum of cut diagrams for the gauge invariant amplitudes $\mathcal{M}_{(a)}$, $\mathcal{M}_{(b)}$, $\mathcal{M}_{(c)}$ and $\mathcal{M}_{(d)}$, but not for each diagram separately.

In addition to the diagrams discussed so far, the amplitude $\pi q \rightarrow (\bar{q}q)q$ receives a contribution from the three-gluon exchange in the t -channel. Such terms can be viewed as belonging to the cut diagrams shown in Fig. 3a in which the hard gluon in the blob is attached to the bottom quark line. We have checked that this extra contribution does not contain the large collinear logarithm $\ln q_\perp^2$ and therefore we neglect it.

3. To start with, consider the calculation of $\mathcal{M}_{(d)}$. Let $l^\mu = \alpha_l p_1^\mu + x_l p_2^\mu + l_\perp^\mu$ be the momentum of the (real) gluon in the intermediate state and let $e^\mu(l)$ be one of the two physical polarization vectors. The two conditions $(e \cdot p_2) = 0$ and $(e \cdot l) = 0$ fix the gauge and result in $e^\mu(l) = e_\perp^\mu + 2p_2^\mu (e_\perp l_\perp) / (\alpha_l s)$.

The effective vertex corresponding to the sum of the three diagrams in Fig. 4 has the form

$$i \frac{g^2 z (z' - z)}{q_\perp^2 z'} \left[\frac{1}{z'} (t^l t^a)_{ij} - \frac{1}{z} (t^a t^l)_{ij} \right] \bar{u}(q_1) \left[\not{v} \not{q}_\perp - 2 \frac{z}{z' - z} (e_\perp b) \right] \frac{\not{p}_2}{s} u(z' p_1). \quad (7)$$

Here t^l and t^a are the $SU(3)$ generators. The color indices l and a belong to the emitted gluon and the t –channel gluon, respectively. We have also introduced an auxiliary two-dimensional vector b^μ defined as:

$$b^\mu = k_\perp^\mu - 2 \frac{(k_\perp q_\perp)}{q_\perp^2} q_\perp^\mu, \quad b^2 = k_\perp^2. \quad (8)$$

Note that the effective vertex, in the limit of small k_\perp , is proportional to $b \propto k_\perp$. The constant terms cancel in the gauge invariant sum of the diagrams in Fig. 4.

[†]The $\mathcal{O}(k_\perp^2)$ behavior can be traced to the gauge invariance of the amplitude, see [8] for the details.

The second effective vertex in Fig. 3d has a similar form. Combining both of them and performing the sum over the polarizations of the emitted gluon we obtain the impact-factor $J_{up}^{(d)}$. Since each effective vertex is proportional to k_\perp , it follows that $J_{up}^{(d)} \sim k_\perp^2$, as expected. The result for the amplitude $\mathcal{M}_{(d)}$ is obtained using the representation in (6). The calculation of $\mathcal{M}_{(c)}$ is very similar. The result for their sum reads:

$$\begin{aligned} \mathcal{M}_{(c)} + \mathcal{M}_{(d)} &= D C_F^2 \int \frac{dk_\perp^2}{k_\perp^2} \int_0^1 dz' \phi_\pi(z') \left(\frac{z \bar{z}}{z' \bar{z}'} + 1 \right) \times \\ &\times \left[\left(\frac{z \bar{z}}{z' \bar{z}'} + 1 \right) + \frac{1}{(N_c^2 - 1)} \left(\frac{z}{z'} + \frac{\bar{z}}{\bar{z}'} \right) \right] \left[\frac{\Theta(z' - z)}{(z' - z)} + \frac{\Theta(z - z')}{(z - z')} \right], \end{aligned} \quad (9)$$

where

$$D = -i s f_\pi \alpha_s^3 \frac{4 \pi^2}{N_c^2 q_\perp^4} \bar{u}(q_1) \gamma_5 \frac{\not{p}_2}{s} v(q_2) \delta_{ij} \delta_{cc'}, \quad (10)$$

and $C_F = (N_c^2 - 1)/2N_c$. The color indices (i, j) correspond to the produced quark-antiquark pair (jets) and (c, c') stand for the color indices of the target quark in the initial and the final state. The contributions $\sim \Theta(z' - z)$ and $\sim \Theta(z - z')$ belong to $\mathcal{M}_{(d)}$ and $\mathcal{M}_{(c)}$, respectively.

For the cut diagrams in Fig. 3a and Fig. 3b we present the final results:

$$\begin{aligned} \mathcal{M}_{(a)} &= -D C_F^2 \int \frac{dk_\perp^2}{k_\perp^2} \int_0^1 dz' \phi_\pi(z') \left(\frac{\bar{z}}{z'} + \frac{z}{\bar{z}'} \right), \\ \mathcal{M}_{(b)} &= D C_F^2 \int \frac{dk_\perp^2}{k_\perp^2} \int_0^1 dz' \frac{\phi_\pi(z')}{z' \bar{z}'} \left[z \bar{z} \left(\frac{\bar{z}}{z'} + \frac{z}{\bar{z}'} \right) + \frac{1}{(N^2 - 1)} \left(\frac{z \bar{z}}{z' \bar{z}'} + 1 \right) \right]. \end{aligned} \quad (11)$$

The transverse momentum integrals $\int dk_\perp^2/k_\perp^2 \sim \ln q_\perp^2$ in (9) and (11) can be identified with the (perturbative) non-forward gluon distributions of a quark:

$$\frac{\alpha_s}{\pi} C_F \int \frac{dk_\perp^2}{k_\perp^2} = \frac{\alpha_s}{\pi} C_F \ln q_\perp^2 \rightarrow {}_q F_\zeta^g(x). \quad (12)$$

To justify this substitution, note that ${}_q F_\zeta^g(x)$ can be calculated to first order in perturbation theory from the evolution equation [5][‡]

$$\begin{aligned} q_\perp^2 \frac{d}{dq_\perp^2} {}_q F_\zeta^g(x, q_\perp^2) &= \frac{\alpha_s}{2\pi} \int_x^1 dz P_\zeta^{gq}(x, z) {}_q F_\zeta^q(z, q_\perp^2), \\ P_\zeta^{gq}(x, z) &= C_F \left[\left(1 - \frac{x}{z} \right) \left(1 - \frac{x - \zeta}{z - \zeta} \right) + 1 \right]. \end{aligned} \quad (13)$$

Using ${}_q F_\zeta^q(z) = \delta(1 - z)$ and taking into account that in the high-energy region $\zeta, x \ll 1$ the quark-gluon kernel simplifies to $P_\zeta^{gq}(x, 1) = 2C_F$, we arrive at the substitution rule in

[‡]In our calculation $F_\zeta(x)$ enters in the DGLAP region $x \geq \zeta$ only, see [5] for more details.

Eq. (12). The final step is to replace ${}_q F_\zeta^g(x)$ by the (nonperturbative) non-forward gluon distribution in the nucleon which is a nontrivial function of the parameters [5]:

$$\langle N(p') | y_\mu y_\nu G_{\mu\alpha}^a(0) G_{\alpha\nu}^a(y) | N(p) \rangle_{y^2 \rightarrow 0} = \bar{u}(p') \not{y} u(p) \frac{(yp)}{2} \int_0^1 dx [e^{-ix(py)} + e^{i(x-\zeta)(py)}] F_\zeta^g(x). \quad (14)$$

Here $G_{\mu\nu}^a$ is the gluon field strength tensor. $u(p)$ and $\bar{u}(p')$ are the spinors of the initial and final nucleons.

Our final result for the imaginary part of the amplitude for dijet production from a nucleon reads

$$\text{Im } \mathcal{M} = -i s f_\pi \alpha_s^2 \frac{4\pi^3}{N_c^2 q_\perp^4} \bar{u}(q_1) \gamma_5 \frac{\not{p}_2}{s} v(q_2) \mathcal{I} \delta_{ij} \quad (15)$$

with

$$\begin{aligned} \mathcal{I} = & \int_0^1 dz' \phi_\pi(z', \mu^2) \left\{ \left[C_F \left(\frac{z\bar{z}}{z'\bar{z}'} - 1 \right) \left(\frac{\bar{z}}{z'} + \frac{z}{\bar{z}'} \right) + \frac{1}{2N_c z'\bar{z}'} \left(\frac{z\bar{z}}{z'\bar{z}'} + 1 \right) \right] F_\zeta(\zeta, \mu^2) \right. \\ & + \left(\frac{z\bar{z}}{z'\bar{z}'} + 1 \right) \left[C_F \left(\frac{z\bar{z}}{z'\bar{z}'} + 1 \right) + \frac{1}{2N_c} \left(\frac{z}{z'} + \frac{\bar{z}}{\bar{z}'} \right) \right] \\ & \times \left. \left[\frac{\Theta(z' - z)}{(z' - z)} F_\zeta \left(\frac{\zeta z'\bar{z}}{z' - z}, \mu^2 \right) + \frac{\Theta(z - z')}{(z - z')} F_\zeta \left(\frac{\zeta \bar{z}'z}{z - z'}, \mu^2 \right) \right] \right\} \end{aligned} \quad (16)$$

The differential cross section summed over the polarizations and the color of quark jets is given by

$$\frac{d\sigma_{\pi \rightarrow 2 \text{ jets}}}{dq_\perp^2 dt dz} = \frac{\alpha_s^4 f_\pi^2 \pi^3}{8N_c^3 q_\perp^8} |\mathcal{I}|^2. \quad (17)$$

The factorization scale μ^2 has to be of order of the transverse momentum of the exchanged gluon. A natural choice is

$$\mu^2 = q_\perp^2 \frac{z'\bar{z}'}{z\bar{z}}. \quad (18)$$

The expression in Eq. (16) presents the main result of this paper.

4. The integrand in (16) is singular at $z' = z$, i.e. when the longitudinal momentum fraction carried by the quark coincides with that of the quark jet in the final state, and at the end-points of the integration region $z' \rightarrow 0$ and $z' \rightarrow 1$. Let us discuss the contributions from these regions in some detail.

The singularity at $z' = z$ is present in the contributions in Fig. 3c,d which include real gluon emission in the intermediate state. The logarithmic integral $\int dz'/|z - z'| \sim \ln s$ is nothing but the usual energy logarithm that accompanies each extra gluon in the gluon ladder. Its appearance is due to the fact the the gluon in Fig. 3c,d can be emitted in a broad rapidity interval and is not constrained to the pion fragmentation region. To

logarithmic accuracy we can simplify the integrand in (16) by assuming $z' = z$ everywhere except for the diverging denominators and the argument of the gluon distribution, to get

$$\mathcal{I}\Big|_{z' \approx z} = 4N_c \phi_\pi(z) \int_z^1 \frac{dz'}{z' - z} F_\zeta(\zeta \frac{z' \bar{z}}{z' - z}, q_\perp^2) \simeq 4N_c \phi_\pi(z) \int_\zeta^1 \frac{dy}{y} F_\zeta(y, q_\perp^2). \quad (19)$$

For a flat gluon distribution $F_\zeta(y) \sim \text{const}$ at $y \rightarrow 0$, and the integration gives $\text{const} \cdot \ln 1/\zeta$ which is the above mentioned logarithm. Note that the color factors combine to produce $C_A = N_c$ signaling that the relevant Feynman diagrams in Fig. 3c,d are those with a three-gluon coupling. Moreover, the factor $2N_c/y$ appearing in (19) can be interpreted as the relevant limit of the DGLAP splitting function [5]

$$q_\perp^2 \frac{\partial}{\partial q_\perp^2} F_\zeta(x = \zeta, q_\perp^2) = \frac{\alpha_s}{2\pi} \int_\zeta^1 dy P_\zeta^{gg}(\zeta, y) F_\zeta(y, q_\perp^2) \simeq \frac{\alpha_s}{2\pi} \int_\zeta^1 dy \frac{2N_c}{y} F_\zeta(y, q_\perp^2). \quad (20)$$

The quantity on the l.h.s. of (20) defines what can be called the unintegrated non-forward gluon distribution and the physical meaning of Eqs. (19) and (20) is that in the region $z' \sim z$ hard gluon exchange can be viewed as a large transverse momentum part of the gluon distribution in the proton, cf. [3]. This contribution is proportional to the pion distribution amplitude $\phi_\pi(z, q_\perp^2)$ and contains the enhancement factor $\ln 1/\zeta \sim \ln s/q_\perp^2$.

Next, consider the contribution to the imaginary part of the amplitude of the dijet production coming from the end-points $z' \rightarrow 0$ and $z' \rightarrow 1$. Summing both of them and using the symmetry of the pion distribution amplitude we obtain

$$\mathcal{I}\Big|_{\text{end-points}} = \left(N_c + \frac{1}{N_c} \right) z \bar{z} \int_0^1 dz' \frac{\phi_\pi(z', \mu^2)}{\bar{z}'^2} F_\zeta(\zeta, \mu^2). \quad (21)$$

Since $\phi_\pi(z') \sim z'$ at $z' \rightarrow 0$, the integral over z' diverges logarithmically. This divergence indicates that the collinear factorization conjectured in (1) is generally not valid. Remarkably, the divergent integral containing the pion distribution amplitude is just a constant and does not involve any z -dependence. Therefore, the longitudinal momentum distribution of the jets in the nonfactorizable contribution is calculable and, as it turns out, has the shape of the asymptotic pion distribution amplitude $\phi_\pi^{\text{as}}(z) = 6z\bar{z}$. The corresponding physical process is the following. The limit $z' \rightarrow 1$ corresponds to a kinematics in which the quark carries the entire momentum of the pion. The fast quark radiates a hard gluon which carries the fraction $(1 - z)$ of quark momentum. This radiation is perturbative and is described by the effective vertex (7) at $z' = 1$. At the final step the hard gluon transfers its entire longitudinal and transverse momentum to the quark jet, and emits a soft antiquark which interacts nonperturbatively with the target proton and the pion remnant. The technical reason for the singularity at $z' \rightarrow 1$ can be traced to the quark propagator whose denominator has the form $\sim 1/[q_\perp^2 \bar{z}'^2/(\bar{z}(\bar{z} - \bar{z}')) - 2\bar{z}'(k_\perp q_\perp)/(\bar{z} - \bar{z}') + k_\perp^2(1 + \bar{z}'/(\bar{z} - \bar{z}')) + i\epsilon]$, where k_\perp is the transverse momentum of the t -channel gluon. In order to extract the leading small- k_\perp

behavior corresponding to the logarithmic collinear divergence we expand this denominator at small k_\perp . The leading term in this expansion cancels in the gauge invariant sum of diagrams, and the second term (linear in k_\perp) plus similar terms from the nominator produce $1/(1-z')^2$. It follows that the divergent logarithm in $\int \phi_\pi(z')/\bar{z}'^2$ is of the form $\ln q_\perp^2/\mu_{\text{IR}}^2$ where μ_{IR} is related to the average transverse momentum of the quarks inside the pion. It is possible that in the case of scattering from a heavy nucleus μ_{IR} may grow as $\sim A^{1/3}$ because of color filtering. A detailed discussion of this effect goes beyond the tasks of this letter.

5. In order to make an estimate we assume that skewedness does not affect significantly the x dependence and adopt the following simple model for the non-forward gluon distribution:

$$F_\zeta(x, \mu) = F_\zeta(\zeta, \mu) \left(\frac{\zeta}{x} \right)^\Delta \quad (22)$$

with $\Delta = 0.3$ [11]. We further notice that at high energies, or at small ζ , there exists a mechanism which effectively suppresses the nonperturbative end-point contributions, or, better to say, enhances the factorizable contributions in comparison to the end-point ones. It is known that in the region of small x the scale dependence of the gluon density $g(x, \mu^2)$ is quite large and can be parametrized by the effective exponent γ : $g(x, \mu^2) = g(x, \mu_0^2)(\mu^2/\mu_0^2)^\gamma$. We take $\gamma = 0.3$ [12] and assume the same scale dependence for the non-forward distribution:

$$F_\zeta(\zeta, \mu^2) = F_\zeta(\zeta, \mu_0^2) \left(\frac{\mu^2}{\mu_0^2} \right)^\gamma. \quad (23)$$

Choosing the scale μ according to Eq. (18) we observe that the end-point singularities (formally) disappear.

The longitudinal momentum fraction dependence of the jets calculated using the expression in (16) and the model for the nonforward gluon distribution in (22), (23) is shown in Fig. 5 for two different choices of the pion distribution amplitude: $\phi_\pi^{\text{as}}(z) = 6z\bar{z}$ and $\phi_\pi^{\text{CZ}}(z) = 30z\bar{z}(2z-1)^2$ [10]. For this plot we have taken $s = 1000$ GeV 2 and $q_\perp = 2$ GeV which roughly corresponds to the kinematics of the E791 experiment [4]. The overall normalization is arbitrary. Notice that the Chernyak-Zhitnitsky (CZ) ansatz for the pion distribution amplitude leads to a much larger (integrated) cross section than the asymptotic distribution[§]. This signals that the leading logarithmic approximation in Eq. (19) is not sufficient and regions of integration in (16) other than $z \approx z'$ play an important rôle. One sees that the sensitivity to the shape of the pion distribution amplitude remains, although there is no direct proportionality as it was assumed in [4].

To summarize, in this letter we have calculated the one-gluon exchange contribution to the imaginary part of the amplitude of pion diffraction dissociation to two jets with large transverse momenta. The answer is given in Eqs. (16), (17) and its main feature is that the jet longitudinal momentum distribution is not simply proportional to the pion

[§]The calculation shown in Fig. 5 serves the illustrative purposes only. In the data analysis one has to take into account that the CZ model [10] is formulated at a low scale and has to be evolved to $\mu \sim q_\perp$ for a meaningful comparison.

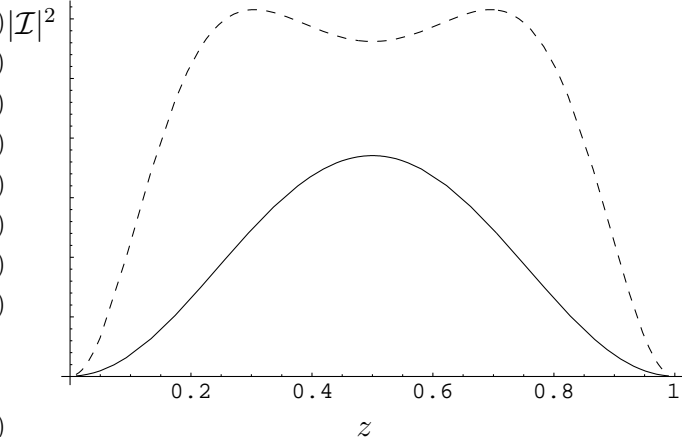


Figure 5: The longitudinal momentum fraction dependence of the jets for two different choices of the pion distribution amplitude: $\phi_\pi^{\text{as}}(z) = 6z\bar{z}$ and $\phi_\pi^{\text{CZ}}(z) = 30z\bar{z}(2z - 1)^2$ shown by the solid and the dashed curve, respectively.

distribution amplitude. The actual dependence is rather elaborate and it has to be taken into account in the data analysis. Our result can be improved by calculating the quark contribution which may be important in the energy range of the E791 experiment and by elaborating on possible nuclear effects that were not taken into account in the present study.

Acknowledgments

We are grateful to L. Frankfurt and A. Radyushkin for discussions and critical remarks. L.Sz. and D.I. were supported by the DFG and the Alexander von Humboldt Stiftung, respectively. V.B. acknowledges warm hospitality at the Institute of Nuclear Theory where this work was finalized.

References

- [1] G. Bertsch, S. J. Brodsky, A. S. Goldhaber and J. F. Gunion, Phys. Rev. Lett. **47** (1981) 297.
- [2] L. Frankfurt, G. A. Miller and M. Strikman, Phys. Lett. B **304** (1993) 1; Found. Phys. **30** (2000) 533 [hep-ph/9907214]; hep-ph/0010297.
- [3] N. N. Nikolaev, W. Schafer and G. Schwiete, Phys. Rev. D **63** (2001) 014020.
- [4] E. M. Aitala *et al.* [E791 Collaboration], hep-ex/0010043.
- [5] A. V. Radyushkin, Phys. Lett. B **385** (1996) 333; Phys. Rev. D **56** (1997) 5524.
- [6] X. Ji, Phys. Rev. Lett. **78** (1997) 610; J. Phys. GG**24** (1998) 1181.
- [7] H. Cheng and T.T. Wu, Phys. Rev. **182** (1969) 1852.

- [8] L.N. Lipatov and G.W. Frolov, Sov. Yad. Fiz. 13, (1971) 588.
- [9] A. V. Efremov and A. V. Radyushkin, Phys. Lett. B **94** (1980) 245; Theor. Math. Phys. **42** (1980) 97;
 G. P. Lepage and S. J. Brodsky, Phys. Lett. B **87** (1979) 359; Phys. Rev. D **22** (1980) 2157;
 S. J. Brodsky, Y. Frishman, G. P. Lepage and C. Sachrajda, Phys. Lett. B **91** (1980) 239.
- [10] V. L. Chernyak and A. R. Zhitnitsky, Nucl. Phys. B **201** (1982) 492. Phys. Rept. **112** (1984) 173.
- [11] L. L. Frankfurt, A. Freund and M. Strikman, Phys. Rev. D **58** (1998) 114001.
- [12] A. D. Martin, M. G. Ryskin and T. Teubner, Phys. Rev. D **55** (1997) 4329.